SPI Conference Proceedings and Reprint Series, Number 10

MONTE CARLO STUDY OF THE TRANSITION FROM COLLISION-DOMINATED TO COLLISIONLESS POLAR WIND FLOW

A. R. Barakat, R. W. Schunk, and I. A. Barghouthi
CASS, Utah State University, Logan, Utah 84322-4405, USA

J. Lemaire
IASB, 3 Avenue Circulaire, B-1180 Brussels, Belgium

ABSTRACT

A Monte Carlo simulation was used to study the flow of H^+ in the polar wind over an altitude range that included the collision-dominated region, the collisionless region, and the transition layer embedded in between. The effects of gravity, polarization electric field, diverging magnetic field, and H^+ –O^+ collisions were considered. In each simulation, 10^6 test H^+ ions were monitored as they diffused across the system and the distribution function, drift velocity, parallel and perpendicular temperatures, and parallel and perpendicular heat fluxes were computed. The flow changes from subsonic to supersonic near the transition layer. The temperature increases with altitude in the collisional region due to frictional heating and then decreases in the collisionless domain due to adiabatic cooling. The heat flux is negative at all altitudes with a minimum near the transition region. In the collisionless region and the transition layer, the shape of the H^+ distribution takes the form of a "kidney bean" embedded in a Maxwellian.

I. INTRODUCTION

The polar wind is an ambipolar outflow of thermal plasma along open field lines at high latitudes. With regard to the behavior of ions, there are two different regions: (1) the collision-dominated region (ion-barosphere), and (2) the collisionless region (ion-exosphere). These two broad regions are separated by a narrow transition layer, where the Knudsen number (ion mean-free-path/electron density scale height) changes rapidly from values much less than one to much greater than one [1]. Different mathematical formulations are needed to study each region. The hydrodynamic models [2] are suitable for studying the collisional region, while the exospheric (collisionless kinetic) models [3–5] are proper for the collisionless region. In principle, the generalized transport models [6, 7] can cover all three regions, but this conjecture has not been thoroughly tested. In the transition layer, a more rigorous mathematical approach should be used [1], such as the Monte Carlo technique.

Yasseen et al. [8] studied the behavior of the photoelectrons in the polar wind. In contrast, our emphasis here is on the behavior of H^+ ions. Barakat and Lemaire [9] used a Monte Carlo simulation to study the flow of a minor species through a background gas and they investigated the effects of mass ratio and inter-particle collision model. However, they did not include body forces acting on the particles between collisions. Here, we use a similar, but modified, code to study the H^+ outflow in the polar wind.

II. THEORETICAL FORMULATION

We consider a three component plasma composed of H^+, O^+, and electrons. The H^+ ions are treated as "test particles", that is, H^+ is minor such that the H^+ self collision is neglected in comparison to the H^+ –O^+ collision, and that the electron density $\simeq$ the O^+ density. The H^+ ions are allowed to diffuse through a background, non-uniform O^+ gas along a radial magnetic flux tube. The effects of gravity, polarization electric field, diverging magnetic afield, and H^+ –O^+ collisions are taken into account. The H^+ –electron collisions are neglected since the ratio of H^+ –electron to H^+ –O^+ collision frequency is as small as the square root of the electron-to-O^+ mass ratio. The electrons are assumed to have a Boltzmann distribution, while the O^+ ions are assumed to have a diffusive equilibrium density distribution as a function of altitude and a corresponding local Maxwellian velocity distribution at each altitude. For simplicity, the electron and O^+ temperatures are assumed to be constant.

The H^+ velocity distribution is governed by the steady-state Boltzmann equation, with allowance for gravity, the Lorentz force, and H^+ –O^+ collisions [10]. With a simple change in variables similar to the one given by [9], this Boltzmann equation can be expressed in terms of a distance that is normalized to the H^+ collisional mean-free-path (mfp),

$$\tilde{z} = \int_r^\infty dr\, \nu(H^+, O^+)/\nu_{th} \tag{1}$$

$$\nu_{th} = [2k\, T(O^+)/m(H^+)]^{1/2} \tag{2}$$

where $\nu(H^+,O^+)$ is the momentum transfer collision frequency given by [10], which varies with altitude.

In the above equations and the presentation that follows, the symbols have the following meaning: n(i), m(i), u(i), T(i), q(i) and f(i) are the density, mass, drift velocity, temperature, heat flux, and distribution function for ion species i, respectively; r is position, k is Boltzmann's constant, and **B** is the magnetic field. The superscripts $\parallel$ and $\perp$ denote directions parallel and perpendicular to **B**, respectively. A ~ over a symbol means it is normalized. The velocity moments are defined in [9]. The normalizations are as follows: the H^+ potential (electrostatic, ϕ_E, and gravitational, ϕ_g) is normalized via $\tilde{\phi} = (\phi_E + \phi_g)/kT(O^+)$; $\tilde{\nu}(H^+) = \nu(H^+)/\nu_{th}$; $\tilde{\mathbf{u}}(H^+) = \mathbf{u}(H^+)/\nu_{th}$; $\tilde{T}_\perp(H^+) = T_\perp(H^+)/T(O^+)$; $\tilde{T}_\parallel(H^+) = T_\parallel(H^+)/T(O^+)$; $\tilde{q}^\perp(H^+) = q^\perp(H^+)/[n(H^+)m(H^+)\, \nu_{th}^{3/2}]$; and $\tilde{q}^\parallel(H^+) = q^\parallel(H^+)/[n(H^+)m(H^+)\, \nu_{th}^{3/2}]$.

III. THE MONTE CARLO MODEL

The model used here is an extension of that used by Barakat and Lemaire [9]. We briefly mention its main features with a special attention given to the

modifications. A simple model for the inter-particle collision is used in this initial study, namely the Maxwell molecule model [9]. The effect of this assumption (and the ones mentioned above) on the results will be discussed in sections IV and V.

Fig. 1 shows the simulation region of length L (30 mfp). The H^+ particles are injected into the system at $\tilde{z} = L$ with a random initial velocity that is consistent with a non-drifting Maxwellian at $\tilde{z} = L + 0$. The time interval between every two successive collisions is randomly generated. Between collisions, the test ion moves under the influence of an effective body force $F_{eff} = -\partial(\phi_g + \phi_E)/\partial\tilde{z}$. The change of the velocity due to collisions is determined randomly. Each test ion is tracked until it exits the system at either $\tilde{z} = 0$ or $\tilde{z} = L$, then another test particle is initiated at $\tilde{z} = L$. The test ions are monitored and the necessary data are accumulated to compute the distribution function and the low order moments (density, drift velocity, parallel and perpendicular temperatures, and parallel and perpendicular heat flows) at given altitudes.

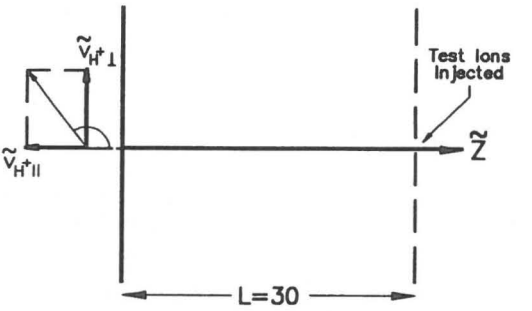

Figure 1. A schematic representation of the model considered by the Monte Carlo method.

We adopt typical values [11] for the O^+ density profile and for the O^+ and electron temperatures (2500 K). The O^+ ions are assumed to be dominant at all altitudes. Combining this assumption with the diffusive equilibrium condition for O^+, we conclude that

$$\phi = \phi_E + \phi_g = -\phi_g\,[0.5\, m(O^+)/m(H^+) - 1] \qquad (3)$$

For simplicity, the modeling is divided into 22 zones where ϕ is approximated by a straight line in each zone. Fig. 2 shows the excellent agreement between the exact value of ϕ (dotted) and the piecewise linear approximation (solid).

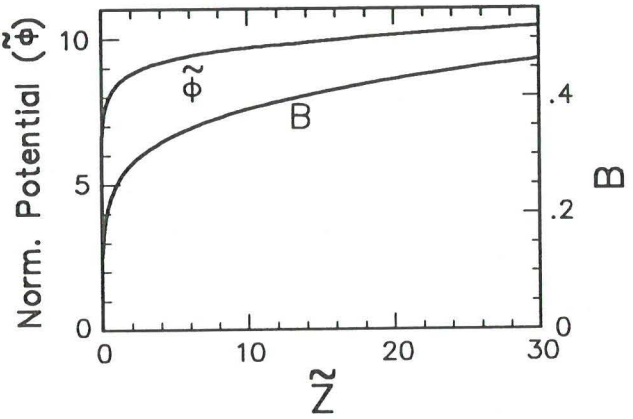

Figure 2. Comparison of the exact profiles (dashed) and the piecewise approximations (solid) adopted in the simulations for the magnetic field and the normalized H^+ potential energy. The exact and approximate profiles are indistinguishable within the graph resolution.

IV. DISTRIBUTION FUNCTION AND ITS MOMENTS

The Monte Carlo technique explained above was used to simulate the behavior of H^+ ions. In each simulation, 10^6 test ions were monitored as they drifted across the system. Subsequently, the H^+ distribution function and its velocity moments were computed at different altitudes. Simulations were conducted both with and without allowance for the **B**-field altitude dependence.

A. No B-Field Altitude Dependence

Fig. 3 shows the H^+ velocity distribution at three altitudes. Deep in the collision-dominated region ($\tilde{z} >> 1$), $f(H^+)$ is very close to Maxwellian with a small drift velocity (Fig. 3c), which is consistent with the assumed conditions at the lower boundary. As altitude increases, $f(H^+)$ becomes increasingly more non-Maxwellian. Roughly speaking, $f(H^+)$ contains two components; a "kidney bean" component (near the maximum of the distribution) which has an upward relative drift, and a Maxwellian-like component (Fig. 3b). As $\tilde{z}$ decreases, the bean-like component becomes more pronounced. At the exobase ($\tilde{z} = 1$) the bean-like component is dominant (Fig. 3b) and in the collisionless region ($\tilde{z} << 1$) the Maxwellian-like component practically disappears (Fig. 3a).

Fig. 4 shows the profiles of the normalized H^+ drift velocity, parallel and perpendicular temperatures, and parallel and perpendicular heat fluxes, as defined in [9]. The drift velocity increases from rather small values to more than 4 (Fig. 4a) as we move from the collision-dominated ($\tilde{z} >> 1$) to collisionless ($\tilde{z} << 1$)

regions. This increase in $\tilde{u}(H^+)$ is due to the increased importance of the body forces (gravitational and electrostatic) acting on H^+ relative to the collisional friction force as altitude increases.

The increase of the drift velocity as the altitude increases (as $\tilde{z}$ decreases from 26 to about 1) results in an increase in frictional heating and, hence, in both $\tilde{T}_{\|}(H^+)$ and $\tilde{T}_{\perp}(H^+)$. However, for $\tilde{z}< 1$ the parallel temperature decreases rapidly as $\tilde{z}\rightarrow 0$ (high altitudes), due to the dominance of parallel adiabatic cooling. According to this process, the parallel velocity dispersion of the particle population should decrease as it is accelerated adiabatically in the

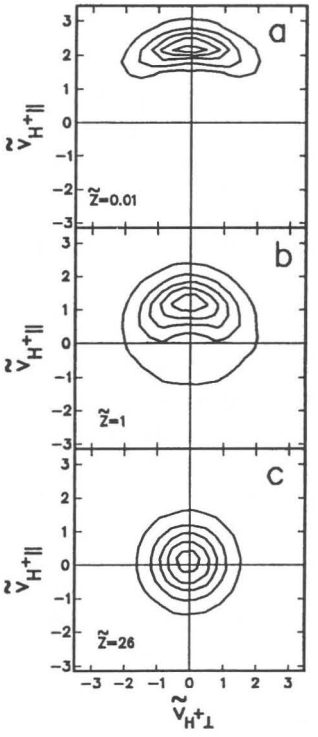

Figure 3. The H^+ velocity distribution function for the case of no B-field altitude dependence and for different values of normalized distance $\tilde{z}$ ($\tilde{z}$ = 26, 1, 0.01). $f(H^+)$ is represented by equal value contours in the normalized velocity.

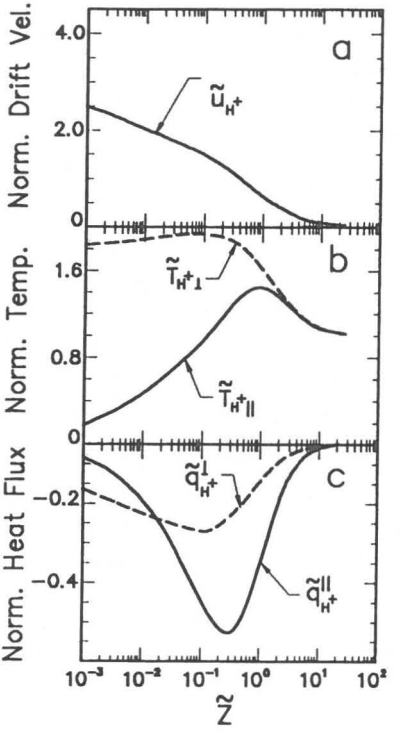

Figure 4. Profiles of H^+ velocity moments for the case of no B-field altitude dependence. These normalized moments are: (a) drift velocity, (b) parallel and perpendicular temperatures, and (c) parallel and perpendicular heat fluxes.

parallel direction. On the other hand, $\tilde{T}_{\perp}(H^+)$ remains almost constant as $\tilde{z} \rightarrow 0$. As discussed later, this results from neglecting the effect of diverging magnetic field lines.

Finally, the heat fluxes are shown in Fig. 4c. In general, both components are downward (negative). This is consistent with the shape of $f(H^+)$ shown in Fig. 3. Deep in the collision-dominated region ($\tilde{z} > 10$) both heat fluxes are very small. As $\tilde{z}$ decreases, they become more negative reaching a minimum of about –0.5 for $\tilde{q}^{\parallel}(H^+)$ and about –0.2 for $\tilde{q}^{\perp}(H^+)$ near the exobase ($\tilde{z} \sim 1$), then their absolute values decrease as $\tilde{z} \rightarrow 0$.

B. B-Field Altitude Dependence Included

We then studied the effect of diverging field lines on the results. In particular, we used the conservation of total particle energy (kinetic + potential) and the first adiabatic invariant to compute the changes in the test particle's velocity between collisions. The profile of B was approximated in a similar way to that of ϕ. Fig. 2 shows the excellent agreement between the exact profile and the piecewise linear approximation. Comparing Figs. 3 and 4 with the corresponding ones with the **B**-field altitude dependence taken into account (not presented here due to space limitations), we find that: (1) The results of the two cases are not significantly different in the low altitude region ($\tilde{z} >> 1$); (2) At $\tilde{z} \approx 0.3$ the perpendicular temperature and heat flux turn around and approach zero as $\tilde{z} \rightarrow 0$ when the **B**-field altitude dependence is included. This is due to the perpendicular adiabatic cooling of the ions as B decreases; and (3) The effect of the altitude dependent **B**-field is such that the distribution function for $\tilde{z} \leq 1$ became closer to a drifting bi-Maxwellian than those shown in Fig. 3.

An ongoing study adopts a more appropriate (Coulomb) collision model. The preliminary results indicate the following: (1) The low order moments (e.g. density and drift velocity) qualitative behavior did not depend on the collision model, while the higher order moments (e.g. heat flow) showed qualitative changes as we adopted the Coulomb collision model. (2) The shape of the distribution function does not depend on the collision model for the collision-dominated and the collisionless regions while it shows a significant variation with the collision model in the transition region.

V. CONCLUSION

A Monte Carlo simulation was used to study the diffusion of H^+ ions under conditions representative of the polar wind plasma. The effects of gravity, polarization electric field, and diverging magnetic field lines were accounted for. The following was found (only the last point is for B = constant):

1. The H^+ flow changes from subsonic in the collision-dominated region ($\tilde{z} >> 1$) to transonic and eventually supersonic at the exobase and in the collisionless region ($\tilde{z} \leq 1$).

2. Both the parallel and perpendicular temperatures increase as $\tilde{z}$ decreases (for $\tilde{z} >> 1$) due to frictional heating. In the collisionless region, both temperatures show a rapid decrease with altitude due to adiabatic cooling.
3. The heat flux components are negative (downward) at all altitudes with minima near the exobase ($\tilde{z} \sim 1$). In comparison with previous works [9], it is clear that the existence of the upward polarization field makes the heat flow significantly more negative.
4. The H^+ distribution function contains two components; a bean-like component, which has a relative upward drift, and a Maxwellian-like component. As $\tilde{z}$ decreases, the bean-like component becomes more pronounced and eventually dominates in the collisionless region ($\tilde{z} << 1$).

Finally, we discuss the assumptions adopted in our model and investigate their potential effects on the results. For simplicity, a Maxwell molecule collision model was used. The preliminary results of an ongoing study show that this assumption has a qualitive effect only on the higher order moments and on the distribution function in the transition region. Also, O^+ was assumed to be the dominant ion, which should be valid for most of the range of $\tilde{z}$ considered here. However, at high altitudes ($\tilde{z} << 1$), H^+ becomes the dominant ion, and consequently, H^+ self-collisions and the dependence of the polarization field on the H^+ density should be considered. Currently, the model is being modified to include such effects and the results will be presented in the future.

REFERENCES

[1] J. Lemaire, J. Atmos. Terr. Phys. **34**, 1647 (1972).
[2] P. M. Banks and T. E. Holzer, J. Geophys. Res. **73**, 6846 (1968).
[3] J. Lemaire and M. Scherer, Rev. Geophys. **11**, 427 (1973).
[4] T. E. Holzer, J. A. Fedder, and P. M. Banks, J. Geophys. Res. **76**, 2453 (1971).
[5] A. R. Barakat and R. W. Schunk, J. Geophys. Res. **88**, 7887 (1983).
[6] R. W. Schunk and D. S. Watkins, J. Geophys. Res. **86**, 91 (1981).
[7] H. G. Demars and R. W. Schunk, J. Geophys. Res. **92**, 5969 (1987).
[8] F. Yasseen, J. M. Retterer, T. Chang, and J. D. Winningham, Geophys. Res. Lett. **16**, 1023 (1989).
[9] A. R. Barakat and J. Lemaire, Physical Rev. A. **42**, 3291 (1990).
[10] R. W. Schunk, Rev. Geophys. Space Sci. **15**, 429 (1977).
[11] P. M. Banks and G. Kockarts, *Aeronomy* (Academic Press, New York, 1973).